

Effect of pH on Catalyst Activity and Selectivity in the Aqueous Fischer-Tropsch Synthesis Catalyzed by Cobalt Nanoparticles

Jorge A. Delgado^{a,b}, Sergio Castellón^c, Daniel Curulla-Ferré^d, Carmen Claver^{a,b}, Cyril Godard^{b*}

^a Centre Tecnològic de la Química de Catalunya, C/ Marcel.li Domingo s/n, 43007, Tarragona, Spain.

^b Departament de Química Física I Inorgànica, Universitat Rovira I Virgili, C/ Marcel.li Domingo s/n, 43007 Tarragona, Spain, Fax: (+34) 977 559563; E-mail: cyril.godard@urv.cat

^c Departament de Química Analítica I Orgànica, Universitat Rovira I Virgili, C/ Marcel.li Domingo s/n, 43007 Tarragona, Spain

^d Total Research and Technology Feluy, Zone Industrielle Feluy C, B-7181 Seneffe, Belgium

Abstract

Cobalt nanoparticles of 2.6 nm were synthesized in water using NaBH₄ as the reducing agent and PVP as stabilizer. The nanoparticles were fully characterized and their catalytic performances evaluated in the aqueous phase Fischer-Tropsch Synthesis (AFTS) at various pH values. The pH of the catalytic solution was shown to affect both the activity and selectivity of the AFTS reaction since side reactions such as WGS and formation of formate from CO₂ were favored at basic pH.

Keywords: cobalt nanoparticles, Fischer-Tropsch, aqueous phase, pH effect

1 Introduction

The increasing worldwide energy demand has made major companies to consider alternative feedstocks such as natural gas, coal and biomass to replace fossil fuels.[1] In this context, the Fischer-Tropsch Synthesis (FTS) has been considered a key process of the biomass-to-liquid (BTL), gas-to-liquid (GTL) and solid-to-liquid technologies (STL)[2] since through this catalytic reaction, syngas can be transformed into high quality synthetic fuels.[3-5] FTS is catalyzed by several transition metals including Ru, Co and Fe. However, Co-catalysts are more attractive from an industrial point of view due to their higher hydrocarbon productivity, good stability and commercial availability.[1]

Currently, the control of the selectivity is one of the main goals in FT investigation.[6] In this context, the use of unsupported nanoparticles is of high interest as they mimic metal surface activation and catalysis at the nanoscale, and shed some light on the effect of the support on catalysis.[7] The first report of the aqueous phase FT synthesis (AFTS) was performed using ruthenium nanoclusters stabilized with poly(N-vinyl-2-pyrrolidone) (PVP) as catalysts.[8] Recently, the effect of the polymer stabilizer was also studied in our group in the AFTS catalysed by RuNPs.[9] PVP stabilized RuNPs were more

active and selective towards hydrocarbons than those stabilized by lignins, indicating that the nature of the stabilizing polymer does affect the catalytic performance in AFTS, strongly influencing the production of CO₂ by Water Gas Shift (WGS) reaction.

One of the earliest studies on colloidal cobalt nanocatalysts applied in the AFTS was published by Kou and co-workers who reported activity of 0.12 mol_{CO}mol_{Co}⁻¹h⁻¹ at 170°C. In this study, the CoNPs were synthesized by chemical reduction using sodium borohydride as reducing agent in water.[10] More recently, the same author compared Co nanoparticles reduced by LiBEt₃H and NaBH₄, in the aqueous-phase Fischer-Tropsch synthesis.[11] Higher catalytic performance was observed for the former case, and comparing the particle size distribution of the catalysts before and after reaction, it was suggested that catalyst reconstruction occurs during the reaction. In addition, the authors proposed that B-doping could affect the catalytic performance of these NPs. They also reported the use of cobalt/platinum alloy nanoparticles stabilized by PVP as catalysts of the AFTS,[12] reaching activity up to 1.1 mol_{CO}mol_{Surf. Co}⁻¹h⁻¹ with a growth factor (α) of 0.8 at 160°C. This outstanding activity was rationalized by the formation of Co overlayer structures on Pt NPs or Pt-Co alloy NPs. Finally, the synthesis of CoNPs by thermal decomposition of Co₂(CO)₈ was also reported using a modified lipophilic C₈-PVP stabilizing agent and squalane as solvent.[13] The resulting CoNPs with a size of 3.54 ± 1.63 nm displayed a FT activity of 0.022 mol_{CO}mol_{Co}⁻¹h⁻¹. Other colloidal Co nanocatalysts for FTS were reported in ionic liquids[14, 15] and squalane[13] although in these cases, low activity and agglomeration issues were described.

In the present work, we describe the synthesis and characterization of colloidal CoNPs stabilized with poly(N-vinyl-2-pyrrolidone) and their evaluation as nanocatalysts in the aqueous phase FT synthesis with a particular focus on the effect of the pH on the catalysts activity and selectivity.

2 Experimental Section

Synthesis of cobalt nanoparticles by chemical reduction method

Cobalt nanoparticles (**Co1**) were synthesized by chemical reduction of cobalt(II) chloride in the presence of polyvinylpyrrolidone as stabilizer (PVP:Co ratio of 20) using sodium borohydride as reducing agent. As a standard procedure, 0.226 g of CoCl₂·6H₂O (0.93 mmol) was dissolved in 50 mL of H₂O containing the 2.066 g of PVP-K30 (18.6 mmol based on monomer units, PVP:Co ratio of 20). Then, a solution of 0.358 g of NaBH₄ (9.30 mmol) in 16 mL of H₂O was added at room temperature during 5 minutes. The solution was maintained under vigorous mechanical stirring for 2 h. Then 100 μL of the colloidal solution was centrifuged, washed with water and re-dispersed by sonication. Three drops of the obtained colloidal solution were deposited on a Cu-formvar or holey carbon grids for TEM and HR-TEM analysis. For the isolation of the CoNPs, the freshly prepared NPs were initially precipitated by a strong magnet and the supernatant was decanted. Then, the precipitated NPs were washed with water to remove the excess of salts and PVP. The decantation and washing process was repeated three

times with water, then three times with ethanol and three times with hexane. The resulted CoNPs were finally dried under vacuum and stored in a glove-box.

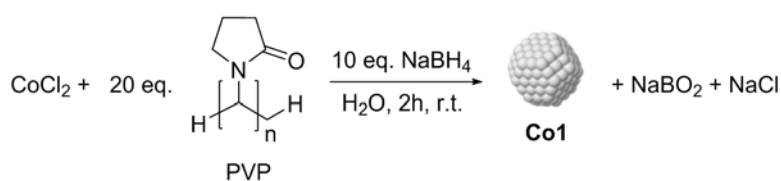
Fischer-Tropsch catalytic experiments

The FT experiments were performed according to reported methods.[8, 9] Freshly synthesized CoNPs (0.93 mmol Co, as described above) were magnetically decanted and washed three times with water and then re-dispersed in 66 ml of water. The obtained suspension of CoNPs was transferred into the autoclave equipped with a Teflon liner. The autoclave was then purged three times with Ar, and pressurized with an Ar pressure of 1.5 bar. 10 bar CO and 20 bar H₂ were further added giving a final pressure of 31.5 bar (H₂:CO:Ar = 2:1:0.15). The autoclave was heated to 180 °C under mechanical stirring at 1000 rpm during 12h. After the reaction, the autoclave was cooled to room temperature prior to gas analysis. All the components contained in the gas phase (CO, H₂, Ar, CO₂, and C₁-C₈ hydrocarbons) were analyzed by GC-TCD and the quantification was performed using calibration curves for each component. The compounds present in the aqueous phase were extracted with dichloromethane (10 ml) containing 1µl of bicyclohexyl as internal standard. The organic phase containing the hydrocarbon and oxygenated products were analyzed by GC-MS. The identification and quantification of products was performed by comparison with standards using calibration curves for each compound.

3 Results and Discussion

3.1. Synthesis and characterization of CoNPs

The CoNPs **Co1** were synthesized by chemical reduction of cobalt chloride in the presence of polyvinylpyrrolidone (PVP) as stabilizer and sodium borohydride as reducing agent (Scheme 1).



Scheme 1. Synthesis of **Co1** by chemical reduction method.

The TEM micrograph and size histogram of **Co1** displayed in Figure 1 showed the formation of spherical cobalt nanoparticles of 2.64 ± 0.92 .

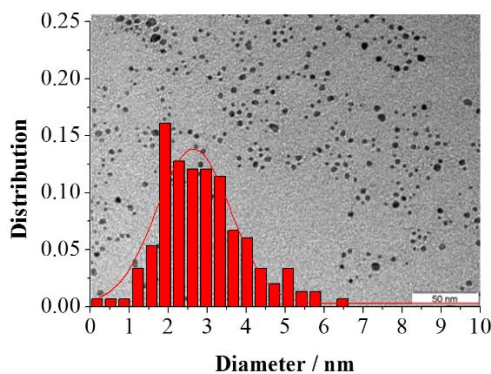


Figure 1. Size histograms and TEM micrographs of **Co1**.

The fine structure of **Co1** was also studied by high-resolution transmission electron microscopy (HR-TEM, Figure 2). In the micrograph, single particles of *ca.* 2.6 nm size were observed, in agreement with the size previously obtained by TEM. The presence of diffuse rings in the electron diffraction pattern of **Co1** also suggested an amorphous structure of the cobalt phase, as previously reported for CoNPs synthesized through similar colloidal methods.[16-18]

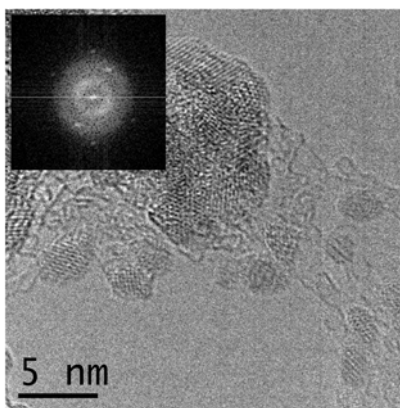


Figure 2. HRTEM image of **Co1** NPs and electron diffraction pattern.

Analysis of the XRD patterns obtained for **Co1** revealed the presence of at least three broad bands centred at 34°, 45° and 60° (Figure 3a), which could not be unambiguously attributed to a specific metallic or oxide phase. Similar XRD patterns were reported for CoNPs synthesized by chemical reduction using NaBH₄ as reducing agent.[18, 19] For instance, Torres et al. reported the synthesis of CoNPs of *ca.* 1 nm exhibiting XRD patterns with broad bands and attributed this effect to the small size of the CoNPs.[19] In contrast, Pileni and co-workers attributed the broadness of XRD patterns of 7 nm CoNPs (also synthesized by chemical reduction) to their amorphous structure.[18] Therefore, in view of these reports, the broad bands observed here could arise from the amorphous structure (in agreement with HR-TEM) and/or due to the small size of the CoNPs.

A sample of **Co1** was subjected to a thermal treatment with the aim to force the crystallization/sintering of the NPs thus revealing a more defined crystalline pattern.[20] **Co1** was heated

to 500 °C within 2-5 min under argon flow and kept at this temperature for 2 h, after which the solid was allowed to rapidly cool to ambient temperature (5-10 min). The diffraction pattern of the thermal treated sample exhibited only fcc and hcp cobalt crystalline phases (Figure 3b). A well-defined pattern of B(OH)₃ was also observed at low angles ($2\theta = 27^\circ$). It was therefore concluded that **Co1** is mainly composed by metallic cobalt and B(OH)₃. The presence of boron was therefore hold responsible for the distortion of the crystalline structure of the CoNPs, as previously reported.[20]

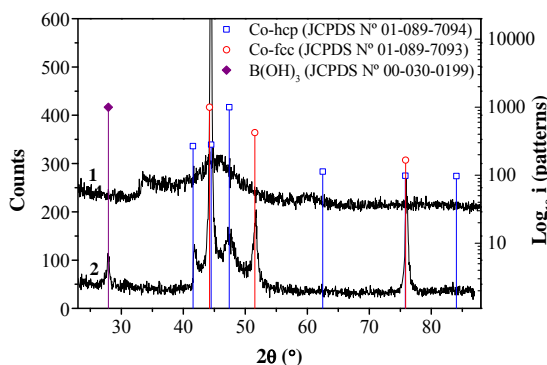


Figure 3. XRD patterns of **Co1** before (1) and after (2) thermal treatment at 500 °C for 2h under argon.

Quantification of the content of cobalt and boron in **Co1** was performed by ICP. The content of Co and B resulted to be 90 and 10 wt% corresponding to a Co/B atom ratio of 2.8. In contrast to our findings, Kou and coworkers reported Co/B values of *ca.* 0.2 for CoNPs of 14 ± 6 nm synthesized under similar conditions.[11] Such low values suggest a considerably higher boron content than that observed for **Co1**, which can be attributed, according to Glavee's report, to the anaerobic conditions used by Kou and co-workers. for the synthesis of CoNPs.[20]

Surface analysis of **Co1** was also performed by X-ray photoelectron spectroscopy (XPS). The full XPS spectra of **Co1** exhibited the presence of Na, Co, O, N, C and B, according to the peaks observed at their characteristic binding energies (1071.6; 781.5; 530.9; 399.2; 284.5 and 191.1 eV respectively, Supporting Information). Deconvolution of the Co 2p_{3/2} spin orbit peaks (Supporting Information) revealed that the reduction degree at the nanoparticle surface is *ca.* 40%. Furthermore, the B 1s XPS spectra of **Co1** exhibited the presence of two bands at 187.97 and 191.6,[21] which were assigned to elemental boron and borates respectively based on reported data (BO₂⁻ BE= 191.8 eV[22]).[23]

Next, the presence of PVP at the surface of these CoNPs was investigated by FTIR and TGA and it was therefore concluded that no PVP is present at the surface of **Co1** after isolation of these NPs.

To summarize, CoNPs with a diameter of 2.6 nm were synthesized by chemical reduction. These CoNPs contained amorphous metallic cobalt, together with some amount of B(OH)₃.

3.2. Fischer-Tropsch catalytic experiments

In order to investigate the effect of the pH in the AFTS, a series of experiments was carried out adjusting the pH of the initial solution to values between 7 and 13.3 *via* the addition of aqueous solutions of NaOH.

Figures 4a and 4b describe the activity and the product selectivity obtained using Co1 as a function of the initial pH. According to Figure 4a, the activity resulted constant from pH 7 to 12.6. For higher pH, an exponential increase up to pH 13.2 was observed ($0.186 \text{ mol}_{\text{CO}}\text{mol}_{\text{Co}}^{-1}\text{h}^{-1}$), however increasing the pH to 13.3 resulted in a decrease of activity ($0.100 \text{ mol}_{\text{CO}}\text{mol}_{\text{Co}}^{-1}\text{h}^{-1}$). In terms of hydrocarbon selectivity, the C_{2+} selectivity decreased from 57 to 10% while the pH increased from 7 to 13.3. It should be mentioned that the hydrocarbons produced under these conditions were always in the C_{2-12} range (Supporting Information). It is noteworthy that the olefin to paraffin ratio (O/P) decreased from 0.8 to 0 with the increase of the initial pH from 7 to 13.2 (Supporting Information).

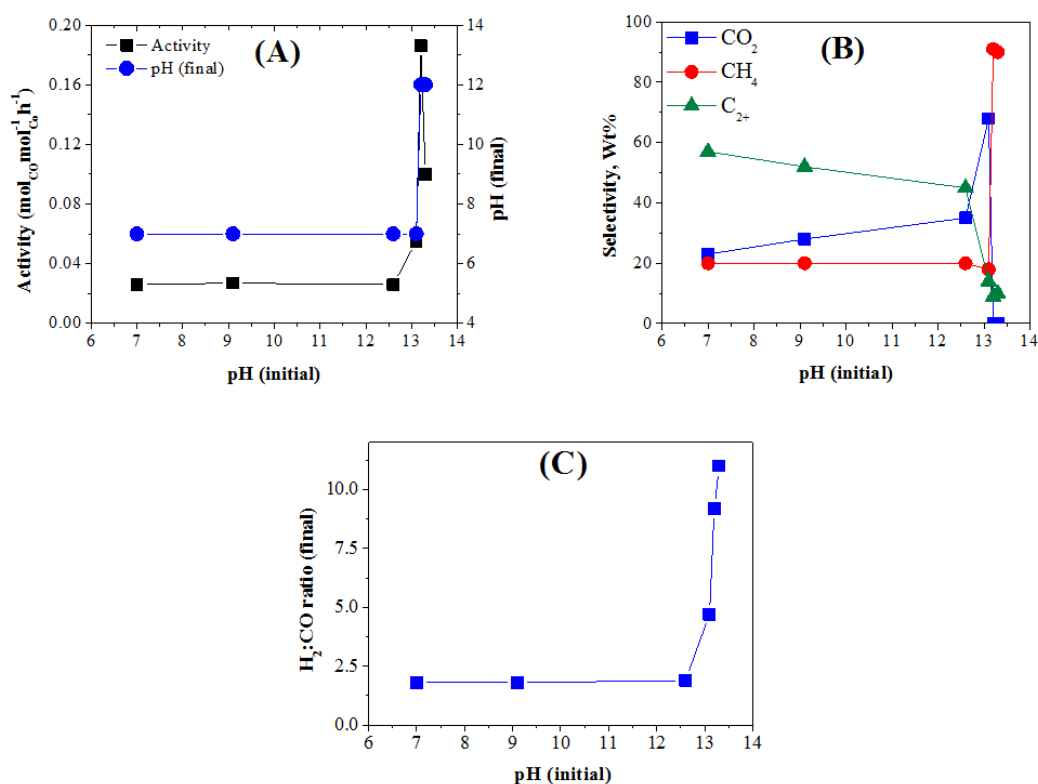


Figure 4. (a) Activity in $\text{mol}_{\text{CO}}\cdot\text{mol}_{\text{Co}}^{-1}\cdot\text{h}^{-1}$, (b) product selectivity in wt% and (c) $\text{H}_2:\text{CO}$ ratio after catalysis of isolated Co1 tested at different pHs.

In contrast, the increase of pH from 7 to 13.1 resulted in the increase of the CO_2 selectivity from 23 to 68%. Curiously, for slightly higher pH (13.3), the CO_2 formation was completely suppressed. The methane selectivity remained constant within the range of pH 7 -13.1, but suddenly increased up to 90% for higher pH. Analysis of the gas phase after catalysis demonstrated that the $\text{H}_2:\text{CO}$ ratio remained constant during catalysis in the range of pH 7-12.6, but increased up to 12 at pH 13.3 (Figure 4c).

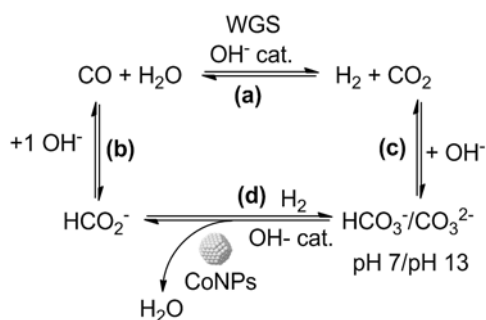
To summarize, the increase in pH caused an increase in H₂:CO ratio during catalysis. An increase in CO₂ selectivity was also observed up to pH= 13.1 but was totally suppressed at higher pH while the CH₄ selectivity increased up to 90%. The higher WGS activity under basic conditions was previously reported in the literature[24, 25] and could explain the initial increase in H₂ and CO₂ concentration. However, the suppression of CO₂ selectivity suggested that this product was transformed under very basic conditions.[26] The increase in CH₄ selectivity was related to the increase in H₂:CO ratio during the reaction, which was reported to favor the methane formation.[27] Such an increase of the H₂:CO ratio favors the formation of methane and paraffins over olefins.

To investigate the possible effect of the pH on the syngas solubility, the solubilities of H₂ and CO in aqueous solutions adjusted at pH 7, 12.6 and 13.3 were measured using the method described by Deimling *et al.*[28] The obtained data demonstrated that in the range of tested pH (7-13.3) the syngas solubility remained constant (Supporting Information). Any participation of the gas solubility in the observed effects in catalysis was thus discarded.

It is well known that the presence of sodium can have a severe effect on FT performances and usually causes significant decrease of the catalytic activity, although no strong effect on the selectivity was reported.[29] Since the base used for these studies was NaOH, the possible influence of sodium on the colloidal catalyst Co1 was evaluated. With this purpose a catalytic experiment was performed under typical FT conditions at pH 11.3 using NH₄OH as the base. Similar results to those with NaOH were obtained and it was concluded that the presence of Na⁺ in the AFTS did not affect the catalytic performances of the CoNPs.

Analysis by ¹³C NMR of the liquid phase after catalysis under basic conditions revealed the presence of formate HCO₂⁻, while carbonate species were not detected (Supporting Information). This observation suggested the possibility of hydrogenation of the carbonate intermediates into formate under FT conditions. To investigate the potential role of the CoNPs as catalysts for this transformation, the direct hydrogenation of HCO₃⁻ to formate was tested in presence of the CoNPs under basic conditions (15 mol% CoNPs; 5.40 mmol NaHCO₃ 10.80 mmol NaOH) and full conversion into formate was observed according to ¹³C NMR analysis of the resulting solution. To the best of our knowledge, this is the first example of carbonate hydrogenation to formate catalyzed by CoNPs. This catalytic transformation has been mainly documented through homogenous organometallic catalysis[30] but there are some reports employing heterogeneous catalysts based on Pd.[31]

It was therefore concluded that the CO₂ produced by WGS under basic conditions reacted with hydroxyl groups to form carbonate which is in turn reduced to formate through hydrogenation catalysed by the CoNPs, as summarized in Scheme 2. Reaction (a) corresponds to the WGS reaction while (b) corresponds to the reaction between CO and hydroxide to yield sodium formate.[32] In path (c), the CO₂ formed from WGS reaction reacts with hydroxide to form carbonate species HCO₃⁻ or CO₃⁻. [33] Finally the carbonate species are hydrogenated into formate in the presence of the CoNPs (path d).



Scheme 2. Proposed pathways for the Co-catalyzed formation of formate from syngas under basic conditions.

4 Conclusions

Small and well defined cobalt nanoparticles (2.6 nm) were synthesized in water using PVP as stabilizer and NaBH_4 as reducing agent. These CoNPs contained amorphous metallic cobalt and some amount of $\text{B}(\text{OH})_3$ and were active in the AFTS. At basic pH, the WGS activity is enhanced thus producing high amounts of H_2 and CO_2 . The increase in H_2 partial pressure resulted in higher selectivity for methane while CO_2 reacted with hydroxide to form carbonate which was subsequently hydrogenated in the presence of CoNPs to form the corresponding formate.

5 Acknowledgements

The authors are grateful to Total S.A., the Spanish Ministerio de Economía y Competitividad (CTQ2013-43438-R, and *Ramon y Cajal* fellowship to C. Godard) and the Generalitat de Catalunya (2014SGR670) for financial support.

References

- [1] V.R. Calderone, N.R. Shiju, D. Curulla-Ferré, S. Chambrey, A. Khodakov, A. Rose, J. Thiessen, A. Jess, G. Rothenberg, *Angew. Chem. Int. Ed.*, 52 (2013) 4397-4401.
- [2] A.Y. Khodakov, *Catal. Today*, 144 (2009) 251-257.
- [3] A. Steynberg. *Fischer-Tropsch Technology. Studies in Surface Science and Catalysis*, Elsevier, 152, Amsterdam, The Netherlands, 2006, pp. 1-3.
- [4] L.P. Dancuart, A. Steynberg, Fischer-Tropsch based GTL technology: a new process?, in: B.H. Davis, M.L. Occelli (Eds.) *Fischer-Tropsch synthesis, catalysts and catalysis*, Elsevier, Eastbourne, UK, 2007, pp. 379-381.
- [5] Q. Zhang, J. Kang, Y. Wang, *ChemCatChem*, 2 (2010) 1030-1058.
- [6] E.F. Sousa-Aguiar, F.B. Noronha, J.A. Faro, *Catal. Sci. Technol.*, 1 (2011) 698-713.
- [7] D. Astruc, F. Lu, J.R. Aranzaes, *Angew. Chem. Int. Ed.*, 44 (2005) 7852-7872.
- [8] C. Xiao, Z. Cai, T. Wang, Y. Kou, N. Yan, *Angew. Chem. Int. Ed.*, 47 (2008) 746-749.
- [9] A. Gual, J.A. Delgado, C. Godard, S. Castellón, D. Curulla-Ferré, C. Claver, *Top. Catal.*, 56 (2013) 1208-1219.
- [10] X.B. Fan, Z.Y. Tao, C.X. Xiao, F. Liu, Y. Kou, *Green Chem.*, 12 (2010) 795-797.
- [11] H. Wang, Y. Kou, *Chin. J. Catal.*, 34 (2013) 1914-1925.
- [12] H. Wang, W. Zhou, J.X. Liu, R. Si, G. Sun, M.Q. Zhong, H.Y. Su, H.-B. Zhao, J.A. Rodriguez, S.J. Pennycook, J.C. Idrobo, W.X. Li, Y. Kou, D. Ma, *J. Am. Chem. Soc.*, 135 (2013) 4149-4158.
- [13] N. Yan, J. Zhang, Y. Tong, S. Yao, C. Xiao, Z. Li, Y. Kou, *Chem. Commun.*, (2009) 4423-4425.
- [14] M. Scariot, D.O. Silva, J.D. Scholten, G. Machado, S.R. Teixeira, M.A. Novak, G. Ebeling, J. Dupont, *Angew. Chem. Int. Ed.*, 47 (2008) 9075-9078.
- [15] D.O. Silva, J.D. Scholten, M.A. Gelesky, S.R. Teixeira, A.C.B. Dos Santos, E.F. Souza-Aguiar, J. Dupont, *ChemSusChem*, 1 (2008) 291-294.
- [16] Chuan Wu, Chun Hui Pang, Feng Wu, Ying Bai, Chi Chen, Y. Zhong, *Adv. Mat. Res.*, 391-392 (2011) 1085.
- [17] M. Mitov, A. Popov, I. Dragieva, *J. Appl. Electrochem.*, 29 (1999) 59-63.
- [18] C. Petit, Z.L. Wang, M.P. Pileni, *J. Phys. Chem. B*, 109 (2005) 15309-15316.
- [19] J. Garcia-Torres, E. Vallés, E. Gómez, *J. Nanopart. Res.*, 12 (2010) 2189-2199.
- [20] G.N. Glavée, K.J. Klabunde, C.M. Sorensen, G.C. Hadjipanayis, *Langmuir*, 9 (1993) 162-169.
- [21] A.Y. Khodakov, W. Chu, P. Fongarland, *Chem. Rev.*, 107 (2007) 1692-1744.
- [22] D.A. Hensley, S.H. Garofalini, *Appl. Surf. Sci.*, 81 (1994) 331-339.
- [23] G.M. Arzac, T.C. Rojas, A. Fernández, *ChemCatChem*, 3 (2011) 1305-1313.
- [24] D.C. Elliott, R.T. Hallen, L.J. Sealock, *Ind. Eng. Chem. Prod. Res. Dev.*, 22 (1983) 431-435.
- [25] D.C. Elliott, L.J. Sealock, *Ind. Eng. Chem. Prod. Res. Dev.*, 22 (1983) 426-431.
- [26] J.B. Tepe, Dodge, B.F., *Trans. Am. Inst. Chem. Eng.*, 39 (1943) 255-276.
- [27] G.P. Van Der Laan, A.A.C.M. Beenackers, *Catal. Rev.*, 41 (1999) 255-318.
- [28] A. Deimling, B.M. Karandikar, Y.T. Shah, N.L. Carr, *Chem. Eng. J.*, 29 (1984) 127-140.
- [29] E. Patanou, A.H. Lillebø, J. Yang, D. Chen, A. Holmen, E.A. Blekkan, *Ind. Eng. Chem. Res.*, 53 (2013) 1787-1793.
- [30] W. Wang, S. Wang, X. Ma, J. Gong, *Chem. Soc. Rev.*, 40 (2011) 3703-3727.
- [31] H. Wiener, J. Blum, H. Feilchenfeld, Y. Sasson, N. Zalmanov, *J. Catal.*, 110 (1988) 184-190.
- [32] M.C. Boswell, J.V. Dickson, *J. Am. Chem. Soc.*, 40 (1918) 1779-1786.
- [33] M. Yoo, S.J. Han, J.H. Wee, *J. Environ. Manage.*, 114 (2013) 512-519.